BME 8 SENIOR CAPSTONE PROJECT

Project Title: Dual Antibody Conjugated Silk Nanoparticles as a Targeted Delivery System for Glioblastoma Multiforme (GBM) Therapy

Team Members: Maddie Yost, Sabrina Zhang, Elysia Chang, Olivia Zeiden
Faculty Advisor: Dr. David Kaplan
Mentor: Sunny Shaidani

Abstract: Glioblastoma Multiforme (GBM) is an aggressive tumor initiated by mutated astrocytes that can be found in the brain and spinal cord. As of now, the current treatment options for GBM are mainly surgery, radiation, and chemotherapy. These are all invasive or have severe side effects, making a targeted delivery system for chemotherapy using antibody-conjugated silk nanoparticles an important avenue to explore. The dual use of antibodies that target EGFRviii and IL-13Rα2 receptors is of interest. EGFRviii is a receptor expressed on the surface of around 30% of GBM cells, and not expressed in healthy brain tissue; IL-13Rα2 is expressed on 75% of GBM cells, but the low-level expression is found in the brain. The goals of this project are to determine the best receptors to target for GBM, determine the appropriate nanoparticle (NP) size for tumor uptake, and induce successful antibody conjugation to the silk nanoparticle surface.

Keywords: targeted therapies, silk nanoparticles, dual antibody conjugation

ELEMENTS OF ENGINEERING DESIGN

What was designed?

The formulation of anti-IL-13Rα2 and anti-EGFRviii conjugated nanoparticles (NPs) to target Glioblastoma Multiforme (GBM) tumor cells was designed. These antibodies bind to IL-13Rα2 and EGFRviii respectively, which are both expressed on the surface of many mutated GBM cells and have little to no expression in healthy brain tissue. The combined use of receptors will reduce off-target interactions and increase the GBM cells targeted in patients. The nanoparticles will be fabricated to be within a 100-120 nm size range for tumor vasculature penetration[1]. A protocol to conjugate antibodies to the silk nanoparticles using EDC/NHS was developed. EDC, in conjunction with NHS, allows for a 2-step coupling of two proteins without affecting the carboxyls of the second protein. Secondary antibodies were used in conjunction with a plate reader and fluorescence microscopy to assess dual antibody conjugation and orientation.

What objectives were set?

The objective of the project was to evaluate an antibody-conjugated silk nanoparticle drug delivery platform as a treatment for GBM. The first objective was to formulate nanoparticles of an appropriate size (100 nm) for tumor infiltration and cell uptake. The second objective was to confirm the singular conjugation of each chosen antibody. The last objective was to dually conjugate both antibodies to the silk nanoparticles and confirm successful conjugation and preservation of antibody binding ability using fluorescence microscopy and plate reading to visualize fluorescence and measure the concentration of the antibody after multiple washes.

How were basic scientific, math, or engineering methods applied?

Silk processing, nanoparticle formation, antibody conjugation, fluorescent imaging, and ultracentrifugation were applied in this project. Concentration calculations, ImageJ image analysis, and PRISM data analysis were utilized to evaluate data.

How were the objectives tested and evaluated?

Our first objective of creating 100 nm nanoparticles was evaluated using Dynamic Light Scattering (DLS). Singular and dual conjugation were confirmed by incubating nanoparticles with fluorescent secondary antibodies, using a plate reader and fluorescent microscopy to visualize and quantify overall binding. Plate reader data and images from dual conjugation was analyzed to quantify overlapping areas of both primary antibody conjugation.

What realistic constraints were considered?

The first constraint was the cost and availability of our chosen antibodies since they are less common and therefore more expensive and harder to acquire than typical antibodies. The second constraint was the limitations of targeted antibody therapies, including off-target interactions. By researching and choosing antibodies with low-level expression outside of GBM tumors, unnecessary exposure to chemotherapy could be reduced. The last constraint was time: there are few papers addressing dual-antibody conjugation, so the ability to successfully do so and develop techniques to evaluate the objectives above may exceed the time limit of one school year.

What alternative solutions were considered?

The decision to target GBM was made after a thorough review of the literature to ensure that it was the best cancer target. The decision to proceed with a dual-targeting NP drug delivery approach and technique, targeting both IL-13Rα2 and EGFRviii, was decided upon after discovering that this approach would allow the project to target a greater population of GBM cells while reducing off-target interactions. Due to shipping constraints, the project was modified

by selecting from available antibodies in the lab. PSTAT3 and anti-rVEGF were chosen due to their relevance in immune suppression and cancer angiogenesis, respectively. An alternative solution if EDC/NHS were to not work would be to try coating the nanoparticles with the antibodies, a process that would involve incubating the nanoparticles in the antibodies diluted with PBS to induce tagging to the surface.

To what extent did the final result meet the set objectives?
While the initial objective of dually conjugating anti-IL-13Rα2 and anti-EGFRviii conjugated nanoparticles to target GBM tumor cells was not designed, a slight modification of the project through the substitution of PSTAT3 and anti-rVEGF allowed for the completion of the project. In that sense, the result met the set objectives as the project was able to prove successful singular and dual conjugated antibodies onto silk nanoparticles to target GBM tumor cells.

DESIGN FLOW CHART

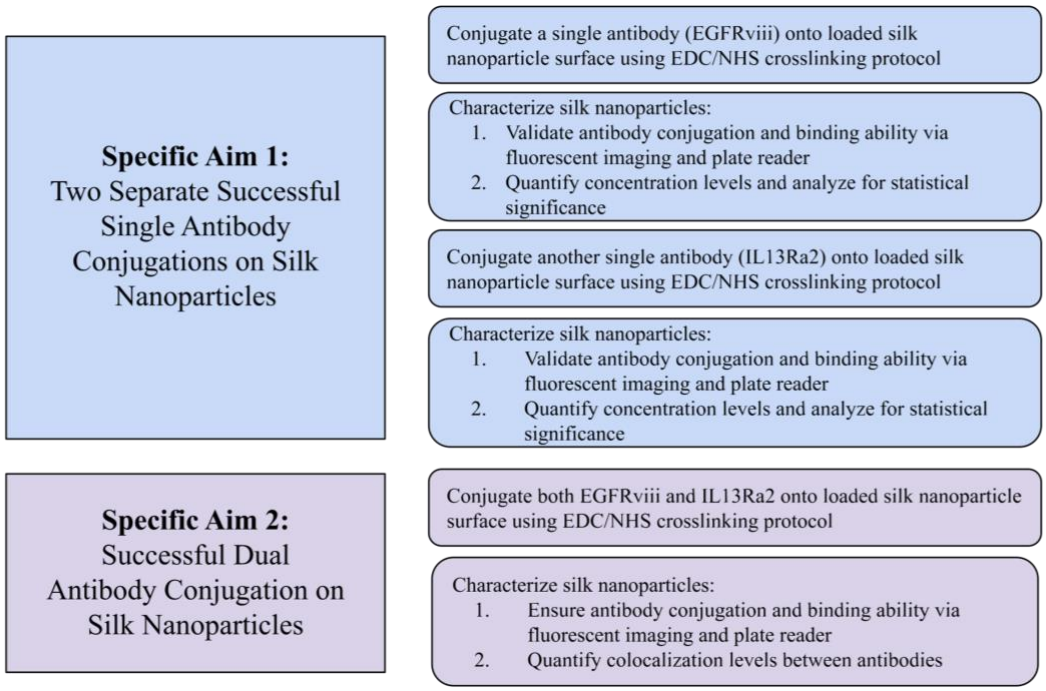

This flowchart outlines the specific aims of the project and the proposed experimental steps to complete each aim. Specific Aim 1 focuses on the singular conjugation of primary antibodies on silk nanoparticles and subsequent validation. Specific Aim 2 centers around dual antibody conjugation and characterization of the silk nanoparticles using various experimental methods.

INTRODUCTION AND BACKGROUND
Glioblastoma Multiforme (GBM) is the most common tumor in the central nervous system (CNS) and accounts for 65% of all CNS malignancies[2]. GBM is one of the most deadly forms of cancer, with a median survival rate of just 12.6 months after diagnosis[3]. Attributing to this severe prognosis is the tumor's location in the CNS means that the blood-brain barrier (BBB) severely limits the delivery of standard therapies[4]. The BBB impedes drug delivery into the CNS, making it nearly impossible for intravenously injected systemic therapeutics like chemotherapies to cross if not modified[5].

Current treatment approaches for glioblastoma involve tumor resection surgery followed by radiation therapy and chemotherapy treatment[6]. Surgery with maximal resection is the goal as 90% resection has been found to increase one-year survival for patients compared to subtotal resections[6]. But tumor resection has been linked to the activation of GBM tumor stem cells and secretion of tumor growth factor, pleiotrophin, leading to tumor recurrence and patient survival is still highly dependent on tumor operability[7]. Radiation targets highly proliferative cancer cells in the tumor microenvironment, inducing double-strand DNA breaks that lead to cell apoptosis[6]. In a study by Piroth et al., radiation therapy was found to only be valuable for patients with complete tumor resection as OS was increased from a median of 8.7 months to 9.5 months, while OS decreased for patients with partial tumor resection and tumor biopsy[8]. Also, most patients are diagnosed with GBM in their 70-80s and radiation therapy is not the most suitable option for elderly patients as age affects treatment efficacy and can increase toxic effects[9]. The chemotherapy used to treat glioblastoma is called temozolomide (TMZ). It is a drug that can penetrate the blood-brain barrier due to its lipophilic properties and can increase patient OS from 2.5 months to 16.2 months[4, 10]. Since chemotherapy is a systemic treatment, off-target effects do occur when other highly proliferative cells in the body are mistakenly attacked. TMZ treatment efficacy could benefit from carrier-like nanoparticles that could enhance tumor targeting ability.

Nanoparticles can mitigate many of the obstacles that currently available therapies cannot overcome. Their advantages include biocompatibility, reduced toxicity, excellent stability, enhanced permeability and retention effect, and precise targeting[11]. The unique targeting ability of these nanoparticles can be enhanced with antibodies that bind to proteins on the surface of the selected cancer cells and deliver the drug of interest.

While nanoparticles can be composed of various materials, silk was selected as the appropriate material due to its biocompatibility, availability, and ease of size optimization and loading[12]. Nanoparticles around 100 nm in the bloodstream are known to be too big to enter healthy tissue but can enter tumors due to their leaky vasculature. Once they have entered the tumor and bound to the cell receptors, they can be endocytosed to deliver the drug. Larger nanoparticles have been found to have longer rates of internalization; therefore, it is advantageous to have a nanoparticle large enough to only target cancerous tissue, yet small enough to be engulfed at an appropriate rate[13].

Epidermal growth factor receptors (EGFR) are transmembrane receptor tyrosine kinases (RTK) and are overexpressed in 50% of glioblastomas[14]. Epidermal growth factor variant three (EGFRviii) is a mutated wildtype EGFR expressed on the surface of GBM cells and commonly associated with GBM. This mutation can lead to continued expression of tyrosine kinases and activate uncontrolled cell proliferation and growth. EGFRviii is expressed in 25-33% of all GBM tumors in patients, and it is not expressed in normal brain tissue[15, 16]. Some studies claim that EGFRviii has never been detected in healthy tissue[16]. Its low expression in normal tissue makes it a suitable target for GBM therapies. Gliomas with EGFRviii have increased Ras activity, Akt/PI3k signaling, and expression of VEGF and IL-8[17]. EGFRviii CAR T cells are in Phase I studies and have shown low off-target toxicity[18].

Interleukin-13 receptor alpha2 (IL-13Rα2) was discovered as a glioma marker in 1995 by the Debinski laboratory[19], since then it has become one of the most studied tumor-specific antigens

in glioblastoma research[20]. IL-13Rα2 is a high-affinity membrane receptor of IL-13 and is expressed in many tumors[21]. It is overexpressed in up to 75% of glioma patients[22]. Healthy expression of IL-13Rα2 is high in the testis and placenta but has low expression in other organs[20]. A phase III trial targeting IL-13Rα2 reported high levels of neurotoxicity due to off-target interactions with IL-13Rα1, a related receptor that is expressed in healthy brain tissue[23]. While this trial revealed the dangers of working with IL-13Rα2, it suggests a promise of an antibody more specific to IL-Rα2 to be found and used. Currently, CAR T-cell therapy targeting IL-13Rα2 is now in Phase I clinical trials[24]. EGFRviii and IL-13Rα2 targeted therapy have both been associated with recurrent antigen loss variants after initial treatment[25].

The combination of two receptor targets would allow for a greater number of GBM cell targets among its heterogeneous population, while also maintaining selectivity and reducing off-target interactions. While this project would have ideally used both EGFRviii and IL-13Rα2, delayed arrival of shipments of these antibodies prohibited these experiments from taking place. Thus, a modification and adjustment were made to use PSTAT3 and anti-rVEGF instead for proof of concept.

Signal transducer and activator of transcription 3 (STAT3) is a transcription factor and a member of the STAT protein family. STAT3 is activated in 60% of primary gliomas and enhanced tumor radioresistance[26]. It is directly involved in the implementation and maintenance of the GBM immunosuppressive microenvironment and plays a central role in many tumors where STAT3 is consistently activated[27]. The expression of STAT3 in GBM tissues is substantially higher than that of normal brain cells. Abnormal activation of STAT3 creates an immunosuppressive tumor microenvironment for GBM. Blocking the STAT3 pathway can effectively inhibit the growth and metastasis of GBM. As such, inhibition of STAT3 may be a new therapeutic approach for GBM, and the combination of STAT3 targeted therapy and conventional therapies may improve the current status of GBM treatment[28].

Vascular endothelial growth factor (VEGF) is the most abundant angiogenesis mediator in glioblastoma and a key driver of their characteristic vasculature[29]. It has been proposed that anti-VEGF agents inhibit the formation of new blood vessels thus inhibiting tumor growth and spread and have been used to treat certain cancers and age-related macular degeneration[30]. Preliminary results from Gerstner et al. found that antibodies that bind VEGF and small molecule tyrosine kinase inhibitors that block receptor activation have prolonged progression-free survival[31]. However, some anti-VEGF therapies have been associated with the development of tumor resistance in GBM patients[32]. Dual conjugation of anti-VEGF with PSTAT3 serves as a mechanism to reduce tumor resistance mechanisms while still targeting tumor angiogenesis. Thus, anti-VEGF agents have been proposed to enhance the survival and quality of life in GBM patients and should be evaluated further[33].

Silk nanoparticles offer a unique opportunity to customize the drug, target, and dose of interest. Silk will be made using a previously established protocol from Kaplan et al. The target size distribution will be around 100-120 nm, based on literature that linked the clinical efficacy of tumor vasculature penetration to this size range[1]. To achieve this size, a silk solution will be produced using 6% concentration, boiled for 30 min, and spun at 500 rpm for nanoparticle formulation. The nanoparticles will be fabricated by solvent emulsion techniques shown in the

methods section, chosen because it allows for precise control over nanoparticle size formation at this range. The size will be measured by dynamic light scattering (DLS), and a distribution of 100-120 nm will be acceptable for further processing. In this project, dual-antibody conjugated nanoparticles will allow for more direct targeting of GBM cells; compared to traditional therapies, a successful formulation will result in more efficacious treatment for better patient outcomes.

UNIFYING FIGURE FOR THE PROJECT

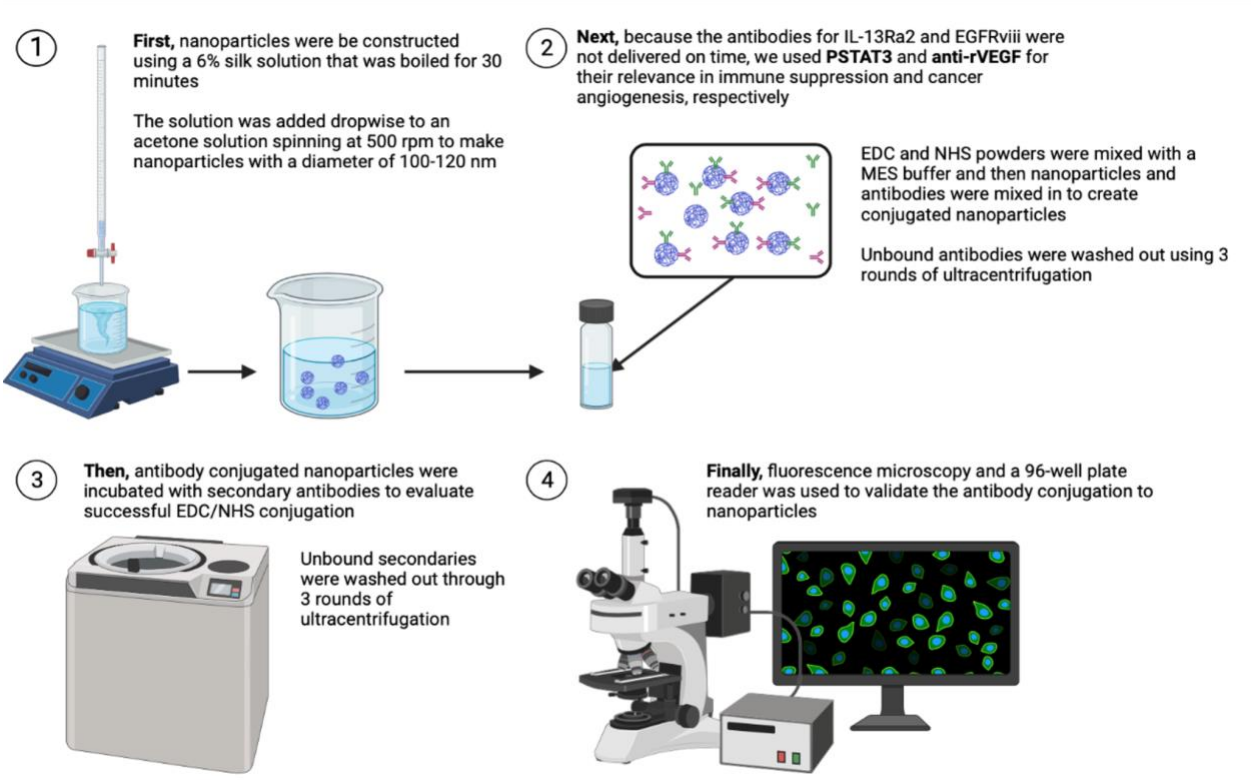

This simple integrated figure visually explains each experimental step of the project. The first step outlines nanoparticle creation. The second step highlights the EDC/NHS process. The third step shows the ultracentrifugation process. The last step depicts fluorescence microscopy and plate reading, two integral steps of our project in finalizing the data collection.

SPECIFIC AIMS, METHODS, AND RESULTS:

Specific Aim 1: Conjugate Anti-EGFRviii and Anti-IL-13Rα2 Separately

In Specific Aim 1, antibodies anti-EGFRviii and anti-IL-13Rα2 will be conjugated onto silk nanoparticles using EDC/NHS conjugation. EDC/NHS was chosen due to its prevalence in literature for analogous platforms. Using EDC/NHS protocols and materials available in the Kaplan Lab, antibodies will be conjugated onto silk nanoparticles in two separate experiments. It is expected that most nanoparticles will be conjugated with the antibodies. We will treat anti-EGFRviii and anti-IL-13Rα2 nanoparticles with secondary mouse and rabbit antibodies respectively and use a Keyence fluorescence microscope to visualize fluorescence that would be present if conjugation to nanoparticles occurred. A plate reader will also be used to determine the concentration of antibody present by measuring the emission and excitation of the fluorescent secondary antibody. Conjugation will be deemed successful based on the visualization of

secondary antibody-tagged nanoparticles compared to that of the control of nanoparticles coated in secondary and the standard curve.

Specific Aim 2: Dual Conjugation of Anti-EGFRviii and Anti-IL-13Rα2

Specific Aim 2 will produce dually conjugated silk nanoparticles with anti-EGFRviii and anti-IL-13Rα2. Dual conjugation was chosen due to previous literature linking it to enhanced therapeutic efficacy in tumor models[34]. We follow EDC/NHS and fluorescence protocols established in Specific Aim 1 to conjugate both anti-EGFRviii and anti-IL-13Rα2 antibodies onto silk nanoparticles as the protocol for dual conjugation is the same as the protocol for single conjugation. We are not expecting that conjugation of one antibody will interfere at all with the conjugation of another due to previous literature in the field. To confirm antibody binding and concentration, the nanoparticles will be treated with secondary mouse and rabbit antibodies for plate reading and fluorescent imaging. It is known that silk nanoparticles experience some small amount of autofluorescence, as silk scaffolds naturally do, so blank nanoparticles with and without secondary antibodies will be used as a control. The fluorescence in each well plate will be qualitatively analyzed in comparison to all conditions. If time allows, anti-IL-13Rα2 and anti-EGFRviii will be bound in different test ratios to determine nanoparticle surface coverage. To start, equal concentrations of each antibody will be tested and adjusted as our experiment progresses.

Methods

Silk Processing[35]

Cut cocoons and remove inside layers, weigh out 4.24g sodium carbonate, and add to 2L of boiling distilled water. Add 5g of cocoons to the solution to degum silk fibers so that sericin is washed away and only fibrin protein remains. Wash degummed silk three times in 1.5L of distilled water, changing the water each time, for 20 minutes each. Remove silk, pull by hand, and air dry inside a fume hood. Add silk into 9.3 M LiBr solution to remove beta sheets and let sit for at least 4 hours in a 60°C oven. Pour dissolved silk into dialysis tubing and place tubing into a 2L beaker of distilled water and spin for 3 days. Change dialysis water 3 times on the first day, twice on the second day, and once on the third day to wash out the LiBr solution. Collect silk solution on day 3 and centrifuge solution twice for 20 minutes at 5-10°C at 9000 rpm, then store in the fridge for up to two weeks. For silk concentration calculations, see Appendix 5.

Silk Nanoparticles[36]

For 6% silk, 500 rpm, 30 min boil, on day 1, add 15-20 mL acetone to labeled small glass jar. Place a 3cm stir bar into the jar and secure the jar onto the center of the stir plate with polymer clay, set to 500 rpm. The vortex created should be centered and no sound should be coming from the stir bar. Measure out 4 mL silk & pour it into a specialized glass dropper. Using the knob on the left side of the glass dropper, twist slowly and carefully (following a titration technique). The solution should drop and fall into the side of the vortex which will help to create the desired nanoparticle size of choice. On day 2, add 2-5 mL of DI water as some of the acetone may have evaporated overnight. For day 3, the final liquid level should be around 4 mL. Move the solution to a 15 mL tube and add DI water up to 10 mL. Clean the sonicator tip with ethanol and hold the 15 mL tube to the sonicator tip. Sonicate at 30% amplitude for 30 seconds 2x and move the tube up and down (without touching the sides or the bottom). Add 300 uL water to the civet and use a p1000 to pipette a drop of the nanoparticle solution. Check the size with the particle solutions app on DLS. For nanoparticle concentration calculations, see Appendix 5.

EDC/NHS[37]

On day 1, reactants can be taken out from the fridge/freezer. EDC and NHS powders are weighed out into small individual jars, respectively. Based on calculations (Appendix 5), the appropriate amount of 0.05 M MES buffer (pH 6) will be added to each to help dissolve the EDC and NHS separately. Calculations will occur to determine the amount of ultrapure water that will be added to the dissolving process (while accounting for the fact that the silk solution already has water in it). In a new jar with a 3cm stir bar, collect 2 mL of silk nanoparticles, MES buffer, EDC +NHS, and 50 uL of the antibody. Set the jar on a stir plate at 200 rpm for 18 hours overnight. On day 2, two tubes with EDC/NHS nano-solution will be filled equally and weighed, using DI water to balance. The ultracentrifuge will be turned on and set to 60K rpm for 30 minutes at 4°C and run with balanced EDC/NHS nano-solutions. The supernatant will be taken out with a needle and resuspended with 3 mL DI water. Repeat two more times (three spins total). Soak the supernatant pellets in 1 mL of DI water and store them in the freezer. For EDC/NHS calculations, see Appendix 5.

Ultracentrifugation[37]

To remove antibodies that were not bound during EDC/NHS, ultracentrifugation of the nanoparticle solution is required. Ultracentrifugation will occur 3 times, and the supernatant from each spin will be collected to use when imaging to determine how much unbound antibody was left in the supernatant, to then help determine how much antibody is bound to the nanoparticles. For detailed directions on each of the 3 spins, refer to Appendix 5.

Secondary Antibody Tagging[38]

Secondary antibody tagging will be used to determine successful EDC/NHS antibody conjugation and orientation. Once thawed at room temperature, nanoparticles will be resuspended in a sealing tube and sonicated. A total of 5 tubes will be generated using nanoparticles, blocking buffer, and secondary antibodies. These 5 tubes will be shaken on a stir plate covered in tin foil for 2 hours before following the **Ultracentrifugation** protocol again. For detailed directions on the preparation of each tube, refer to Appendix 5.

Imaging

To validate the antibody conjugation, fluorescence microscopy and a 96-well plate reader were utilized. Nanoparticles will express fluorescence, but it is important to note that some of it may also be attributed to silk-autofluorescence. Imaging will help us validate whether the conjugation was completed successfully. For detailed directions and a step-by-step protocol, refer to Appendix 5.

Results

Over the course of the year, five batches of silk nanoparticles were produced. Each batch was created with 6% silk and spun at 500 rpm, and the silk used was boiled for 30 minutes according to the protocol to obtain particles around 110.43 nm in size[39]. Dynamic light scattering (DLS) particle size distribution analysis showed particles were 96.86 nm, 72.00 nm, 70.00 nm, 77.97 nm, and 74.50 nm.

EDC/NHS was performed on these nanoparticles despite the size deviating from our desired 100 nm nanoparticles. An initial proof of concept experiment on IL-4 antibodies for single antibody

silk conjugation was performed and deemed successful. After tagging IL-4 conjugated nanoparticles and control blank nanoparticles with red anti-rat AlexaFluor 594 secondary antibody, samples were analyzed via plate reader and Keyence fluorescence microscope. Figure 1 below shows that quantitatively, antibody concentration was significantly greater in the sample group of nanoparticles conjugated with IL-4. Visually, figure 1A has more red signals, while Figure 1B has fewer, yet larger, aggregates of red. This suggests IL-4 conjugation was successful and results are not skewed by auto-fluorescence or off-target binding.

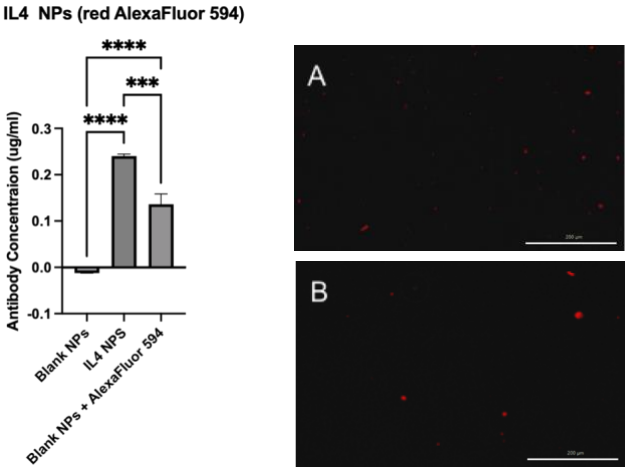

Figure 1. Antibody concentrations of blank NPs, blank NPs incubated with secondary antibody, and IL-4 conjugated NPs incubated with secondary antibody. (n=3; **** $p<0.0001$; *** $p = 0.0002$). (A) IL-4 conjugated NPs and (B) blank NPs incubated with AlexaFluor 594 were imaged using a Keyence fluorescence microscope.

PSTAT3 and anti-rVEGF were then selected from a list of available antibodies in the lab to continue forward with dual conjugation experiments as anti-EGFRviii and anti-IL13-Ra2 were not delivered on time. PSTAT3 and anti-rVEGF were chosen due to their relevance in immune suppression and cancer angiogenesis, respectively[40]. Three rounds of EDC/NHS were performed on single conjugated PSTAT3, single conjugated anti-rVEGF, and dual conjugated PSTAT3 and anti-rVEGF nanoparticles. To identify the conjugated nanoparticles, each particle was tagged along with blank particle controls using either a red anti-rat AlexaFluor 594 secondary antibody, a green anti-rabbit AlexaFluor 488 secondary, or both. The samples were then analyzed using a Keyence fluorescence microscope and a plate reader. Figure 2 depicts acquired images from the Keyence fluorescence microscope. Figure 2A is an overlay of the green and red fluorescence of the dual conjugated nanoparticles, with yellow/brown indicating the presence of both PSTAT3 and anti-rVEGF. Figure 2B portrays a single conjugated PSTAT3, tagged with a green secondary antibody, and Figure 2C portrays a single conjugated anti-rVEGF, tagged with a red secondary antibody. Both images indicate the presence of cell aggregates specific to either PSTAT3 or anti-rVEGF conjugated nanoparticles. Finally, Figures 2D, 2E, and 2F show images of three control conditions of blank nanoparticles tagged with green AlexaFluor 488 secondary (2E), red AlexaFluor 594 secondary (2F), or both secondaries (2D) as comparison points. The visual difference in signals between the conjugated groups (2A-C) and the blanks (2D-F) supports the claim that the fluorescent signals are the result of specific antibody binding rather than off-target binding or autofluorescence.

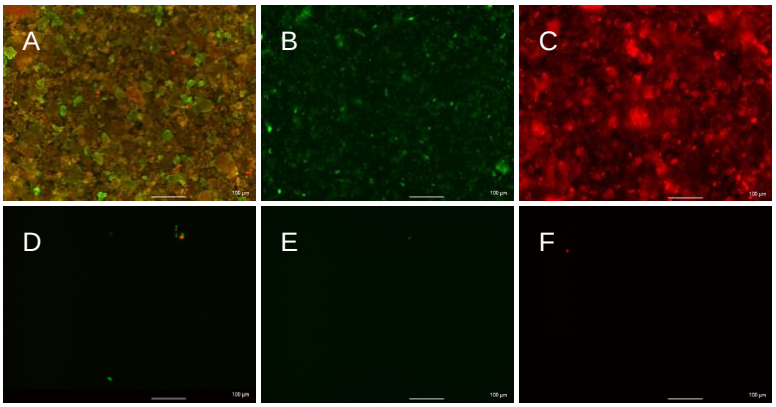

Figure 2. Green anti-rabbit AlexaFluor 488 binds to PSTAT3, and red anti-rat AlexaFluor 594 binds to anti-rVEGF. (A) Dual PSTAT3/anti-rVEGF conjugated NPs tagged with AlexaFluor 488 and AlexaFluor 594; (B) single PSTAT3 conjugated NPs tagged with AlexaFluor 488; (C) single anti-rVEGF conjugated NPs tagged with AlexaFluor 594 were fluorescently imaged. Blank NPs were tagged with (D) AlexaFluor 488 and AlexaFluor 594; (E) AlexaFluor 488; (F) AlexaFluor 594.

Further analysis of the images in Figure 2 resulted in the superimposed white area for better visualization of the overlap between PSTAT3 and anti-rVEGF. Figure 3 provides a visual of image processing for calculating the overlap and colocalization of the two antibodies. The white area makes the area of overlap between PSTAT3 and anti-rVEGF clearer and superimposing the white over the dual (Figure 3D) and single layers (Figure E, F) of the fluorescent signal allows the viewer to see that a significant portion of the area where one antibody is present, the other is also present. Table 1 further analyzes this relationship by calculating the relative area of green fluorescence (Figure 3B), red fluorescence (Figure 3C), and the white area of overlap imposed upon the images. By dividing the relative area of overlap by the relative area of the green or red signal, it was found that 80.969% of PSTAT3 was colocalized with anti-rVEGF, and 82.012% of anti-rVEGF was colocalized with PSTAT3.

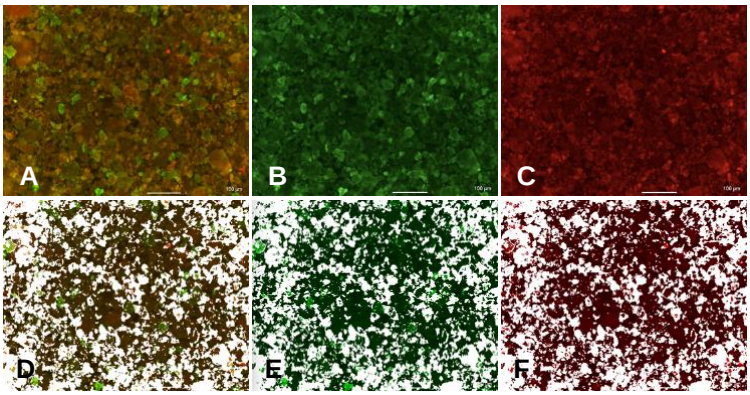

Figure 3. Fluorescence images of NPs dually conjugated with PSTAT3 and anti-rVEGF. Red signifies the presence of anti-rVEGF and green signifies the presence of PSTAT3. Image processing with ImageJ superimposed white where red and green signals overlap. (A) shows the overlay of PSTAT3 and anti-rVEGF presence on the NPs, and (B) and (C) show the PSTAT3 and anti-rVEGF layers separated from each other. (D-F) illustrate the areas in white in which PSTAT3 and anti-rVEGF overlap.

Area of PSTAT3	39.326
Area of anti-rVEGF	38.826
Area of overlap	31.842
overlap/PSTAT3	**80.969%**
overlap/anti-rVEGF	**82.012%**

Table 1. ImageJ Analysis of images in Figure 3 calculated relative areas of overlap as well as green and red fluorescent signals for PSTAT3 and anti-rVEGF respectively. 80.969% of PSTAT3 was colocalized with anti-rVEGF, and 82.012% of anti-rVEGF was colocalized with PSTAT3.

Figure 4 shows that antibody concentrations of dually conjugated PSTAT3 and anti-rVEGF nanoparticles tagged with green AlexaFluor 488 (4A) and red AlexaFluor 594 (4C) were statistically significant as compared to blank nanoparticles and the secondary incubated blank nanoparticles controls. Additionally, single conjugated PSTAT3 (4B) and anti-rVEGF (4D) nanoparticles were also found to be significantly different from their blank nanoparticle and secondary incubated nanoparticle controls. This provides quantitative support that PSTAT3 and anti-rVEGF were successfully conjugated to silk nanoparticles--both dually and individually. Antibody concentrations were extrapolated from standard curve data of green AlexaFluor 488 and red AlexaFluor 594. Additional experimental replicates were conducted by Sunny Shaidani to augment the data set (Figure 4B), allowing for more precise quantification of antibody concentration significance. Qualitative differences observed via fluorescence microscope (Figure 2) support the quantitative findings of successful dual and single conjugation (Figure 4).

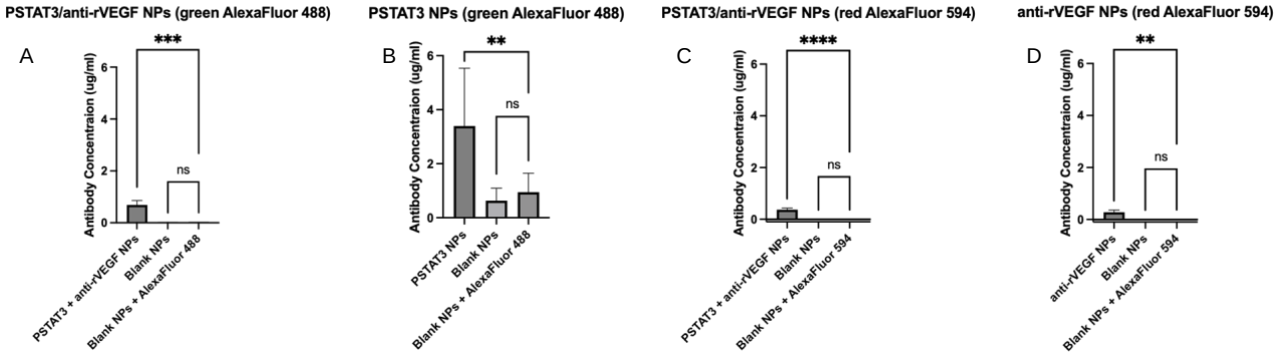

Figure 4. Antibody concentrations of (A) dual conjugated PSTAT3 and anti-rVEGF NPs tagged with green AlexaFluor 488, (B) single conjugated PSTAT3 NPs tagged with green AlexaFluor 488, (C) dual conjugated PSTAT3 and anti-rVEGF NPs tagged with red AlexaFluor 594, (D) single conjugated anti-rVEGF NPs tagged with red AlexaFluor 594 compared to blank NPs and blank NPs incubated with their respective secondary antibodies. Tukey's multiple comparisons test on ordinary one-way ANOVA was used to statistically analyze the data. (A, C, D n=3; B n=9; ** p=0.0006; ***p=0.0002;****p<0.0001)

DISCUSSION AND FUTURE WORK

Discussion

GBM is a deadly cancer affecting the CNS with very low survival rates and few treatment options. This study sought to create a novel therapy system for better patient prognosis. To create a new treatment platform, a novel dual conjugated silk nanoparticles delivery system was created using EDC/NHS techniques and analyzed using fluorescent microscopy and plate reader data. The results of this data suggest successful conjugation of primary antibodies as evidenced by fluorescent secondary antibody tagging.

Silk nanoparticles with a diameter between 70-80 nm were used for EDC/NHS conjugation. While these nanoparticles fell short of the 100 nm target diameter size, this variation does not affect the efficacy of EDC/NHS conjugation or the subsequent results. Singular conjugation proof of concept was performed using an IL-4 primary antibody. Primary antibodies were determined to be conjugated successfully in the correct orientation when secondary antibodies

were able to bind to the antigen site on the primary antibody and fluoresce. The fluorescence was then checked and compared against blank nanoparticles and blank nanoparticles incubated with secondary antibodies. This was to confirm that any fluorescence was only due to proper secondary binding and not influenced by silk autofluorescence or non-specific secondary coating respectively. Antibodies that were improperly conjugated would not have their binding site available for secondary binding thus they would not fluoresce. PRISM analysis of plate reader data using one-way ANOVA and Tukey's multiple comparison tests found insignificant levels of non-specific coating and silk autofluorescence. The greatest fluorescence was still from secondary binding to the IL-4 antibody. This confirmed that the antibody was present and in the correct orientation for binding. The final concentration of the IL-4 conjugated nanoparticles tagged with secondary was lower than the initial concentration added during EDC/NHS. This suggests that only a portion of the IL-4 antibody was conjugated onto the nanoparticle surface during EDC/NHS. It is possible that some conjugated antibodies were pulled off the nanoparticle surface during ultracentrifugation, as the concentration of antibodies in the supernatants increased with the number of washes.

Singular silk nanoparticle conjugation was repeated with PSTAT3 and anti-rVEGF. Experimental replicates were used to further develop the data set and create a stronger statistical analysis of the antibody concentration. Plate reader data was analyzed in PRISM using one-way ANOVA and Tukey's multiple comparison tests and found that single conjugation of PSTAT3 and anti-rVEGF, respectively, were significantly different as compared to the controls (Figure 4). Once again, this confirmed that each antibody was present and in the correct orientation for binding.

Dual conjugation of silk nanoparticles with PSTAT3 and anti-rVEGF was assessed using plate reader data and a Keyence fluorescence microscope. Analysis of plate reader data confirmed statistically greater antibody concentrations of both PSTAT3 and anti-rVEGF in dual conjugated nanoparticles. Furthermore, quantitative findings from data analysis (Figure 4) are also qualitatively observed via the Keyence microscope (Figure 2). Image analysis of dual conjugated nanoparticles found that 80.969% of PSTAT3 was colocalized with anti-rVEGF, and 82.012% of anti-rVEGF was colocalized with PSTAT3 (Appendix 5). The high levels of colocalization suggest that PSTAT3 and anti-rVEGF can likely be found on the same individual nanoparticle, thus completing the objective of dual conjugation of two antibodies onto a single nanoparticle. However, this also suggests that there remains a small population of nanoparticles with only one antibody type, or no antibodies conjugated to its surface, an issue that future projects can address through nanoparticle isolation. The visualized nanoparticle aggregates in Figure 3 further support the successful conjugation of both PSTAT3 and anti-rVEGF. ImageJ software was utilized to find that the green fluorescence had a relative area of 39.326 and red had that of 38.826, suggesting similar conjugation success of PSTAT3 and anti-rVEGF antibodies (Table 1).

It is important to note that there are some limitations to this study. Firstly, nanoparticles observed during fluorescent imaging were still aggregated despite several rounds of sonication before imaging, hindering the characterization of singular nanoparticles. Secondly, clinical relevance was unable to be established during this round of experimentation as timing did not permit cell uptake studies. However, both points can be ameliorated with future work. Furthermore, some differences in antibody concentrations between samples can be attributed to differences in

resuspension and washing during rounds of ultracentrifugation; however, this can be addressed in the future with replicate studies to minimize the spread of data and gain stronger data.

Future Work

This study provides a proof of concept for the novel dual-conjugation of silk nanoparticles; however, more can still be done. Future work could conduct additional replicate studies including using IL-13Rα2 and anti-EGFRviii, testing the targeting ability in a relevant cell model, developing a more robust conjugation validation method, and repeating the experiment with other relevant GBM targets.

Replicate studies using anti-IL-13Rα2 and anti-EGFRviii are specifically relevant due to their prevalence in GBM patients and low expression and healthy tissues. In addition, future studies should consider using flow cytometry to isolate U87 cells with target receptors for in vitro testing of uptake. Eventually, silk nanoparticles should be fabricated with a doxorubicin core and targeting can be tested using a live/dead assay for treatment efficiency and feasibility.

Future research should also consider using other antibody conjugation techniques to validate dual conjugation on a single nanoparticle. Further validation of conjugation can be conducted using in-house ELISA kits to target anti-IL-13Rα2 and anti-EGFRviii ELISA kits. Additionally, previous studies have used X-Ray photon spectrometry as well as direct protein assays to further corroborate if antibodies are conjugated to the same nanoparticle. Though it is challenging to detect due to a high concentration of nanoparticles in the image making it tricky to evaluate individual nanoparticles, colocalization numbers of 80.969% and 82.012% suggest that a portion of the nanoparticles either have only one type of antibody or no antibody bound to its surface. In the future, isolating and removing any unbound nanoparticles using flow cytometry cell sorting should be conducted. Additionally, other studies should focus on how to optimize the silk nanoparticle formulation protocol to ensure 100-120 nm nanoparticles in every experiment.

Finally, future experiments could use different antibodies specific to GBM to find other relevant therapeutic models. EphA2 is another relevant target overexpressed in GBM and found to be elevated in approximately 90% of GBM specimens, thus it represents a new marker and novel target for the development of molecular therapeutics against GBM. Otherwise, continuous testing on IL-13Rα2 and EGFRviii would be key to exploring the use of dual conjugated silk nanoparticles as a targeted delivery system for GBM therapy. Eventually, live testing of these nanoparticles on U87s isolated to express IL-13Rα2 and EGFRviii would be beneficial to see if the antibodies on a heterogeneous GBM cell line can be dually conjugated to establish clinical relevance.

<u>CONCLUSION</u>

- Our experiments have produced a novel proof of concept for dual antibody conjugated silk nanoparticles
- Silk nanoparticles formed using the 6% silk solution, 30-minute boil, 500 rpm protocol were consistently smaller than the goal 100-120 nm diameter nanoparticles expected as multiple replicate experiments created 70-80 nm diameter nanoparticles

- EDC/NHS successfully modifies the surface chemistry of silk nanoparticles, allowing for antibody conjugation
    - IL-4 was successfully conjugated to the surface of silk nanoparticles
    - PSTAT3 and anti-rVEGF were successfully conjugated to silk nanoparticles both individually and together
- The presence of correctly oriented primary antibodies on the surface of silk nanoparticles was determined through the binding of secondary antibodies Alexa Fluor 594 (IL-4, anti-rVEGF) and Alexa Fluor 488 (PSTAT3)
- Secondary antibody fluorescence was properly visualized using Keyence fluorescence microscopy and quantified using a plate reader
- Based on high levels of colocalization determined through ImageJ analysis of fluorescent images, dual antibody conjugation on individual nanoparticles' surfaces is predicted
- To confidently determine and quantify the presence of antibodies on the surface of silk nanoparticles, a validation technique should be created similar to that of a direct protein assay
- This study was a proof of concept for dual antibody conjugated silk nanoparticles because GBM tumor specific antibodies were not delivered on time to be used in the project
- Future experiments should focus on using GBM tumor specific antibodies, like EGFRviii and IL-13Rα2, and studying nanoparticle cellular uptake using 2D GBM cell culture

INDIVIDUAL CONTRIBUTIONS

- **Maddie Yost**: GBM lit review research, antibody (EGFRviii) lit review research, lead silk processing, and cell culture training for a group, added to/edited all Biweekly reports and Technical Reports/Presentation, Zoom meeting with Dr. Saul Priceman, sonication training with Sunny, led ultracentrifugation training, created storyline for K-12 poster, nanoparticle creation, ultracentrifugation, imaging, Google Sheets data analysis, edited Final Technical Report and Design Day 40x30 Poster
- **Olivia Zeiden**: GBM lit review research, Breast cancer lit review (ruled out), silk processing, sonication & nanoparticle training, added to/edited all Biweekly reports and Technical Reports/Presentation, updated project timeline with relevant dates and aims, EphA2 Antibody lit review, Zoom meeting with Dr. Saul Priceman, continued contact with Saul Priceman about cell lines, animated K-12 poster, nanoparticle creation, ultracentrifugation, imaging, edited Final Technical Report and Design Day 40x30 Poster, Edited and updated website
- **Sabrina Zhang**: GBM lit review research, hepatocellular carcinoma (ruled out) lit review, silk processing and U87 cell culture training, nanoparticle training, edited project schedule, added to/edited all Biweekly reports and Technical Reports/Presentation, lit review for IL-13Rα2 as potential target, Zoom meeting with Dr. Saul Priceman, sonication & DLS training, set up order form for antibodies, found 2 EDC/NHS kits for potential use, nanoparticle creation, ultracentrifugation, imaging, Prism 9 data analysis, ImageJ image and data analysis, edited Final Technical Report and Design Day 40x30 Poster
- **Elysia Chang**: GBM lit review research, silk processing and cell culture, nanoparticle training, added to/edited all Biweekly reports and Technical Reports/Presentation, created project timeline, HCC initial research (ruled out), EGFRv3 research, Zoom meeting with Dr. Saul Priceman, sonication & DLS training, nanoparticle creation, ultracentrifugation,

imaging, EDC/NHS, created/edited website, animated K-12 poster, edited Final Technical Report and Design Day 40x30 Poster

ACKNOWLEDGEMENTS

Many thanks to Dr. David Kaplan, Dr. Joseph Brown, Olivia Foster, and the Tufts Department of Biomedical Engineering for providing us with the opportunity to conduct research. A special thank you to Sunny and Charlotte for taking the time out of their busy schedules to mentor us. We could not have done it without them.

REFERENCES

(1) Madhankumar, A. B.; Slagle-Webb, B.; Mintz, A.; Sheehan, J. M.; Connor, J. R. Interleukin-13 receptor–targeted nanovesicles are a potential therapy for glioblastoma multiforme. *Molecular Cancer Therapeutics* **2006**, *5* (12), 3162-3169. DOI: 10.1158/1535-7163.Mct-06-0480 (acccessed 11/3/2022).

(2) Ellsworth, S.; Ye, X.; Grossman, S. A. Clinical, Radiographic, and Pathologic Findings in Patients Undergoing Reoperation Following Radiation Therapy and Temozolomide for Newly Diagnosed Glioblastoma. *Am J Clin Oncol* **2017**, *40* (3), 219-222. DOI: 10.1097/coc.0000000000000136 From NLM.

(3) Carlsson, S. K.; Brothers, S. P.; Wahlestedt, C. Emerging treatment strategies for glioblastoma multiforme. *EMBO Mol Med* **2014**, *6* (11), 1359-1370. DOI: 10.15252/emmm.201302627 From NLM.

(4) de Gooijer, M. C.; de Vries, N. A.; Buckle, T.; Buil, L. C. M.; Beijnen, J. H.; Boogerd, W.; van Tellingen, O. Improved Brain Penetration and Antitumor Efficacy of Temozolomide by Inhibition of ABCB1 and ABCG2. *Neoplasia* **2018**, *20* (7), 710-720. DOI: 10.1016/j.neo.2018.05.001 From NLM.

(5) Pourgholi, F.; Hajivalili, M.; Farhad, J. N.; Kafil, H. S.; Yousefi, M. Nanoparticles: Novel vehicles in treatment of Glioblastoma. *Biomed Pharmacother* **2016**, *77*, 98-107. DOI: 10.1016/j.biopha.2015.12.014 From NLM.

(6) Tan, A. C.; Ashley, D. M.; López, G. Y.; Malinzak, M.; Friedman, H. S.; Khasraw, M. Management of glioblastoma: State of the art and future directions. *CA Cancer J Clin* **2020**, *70* (4), 299-312. DOI: 10.3322/caac.21613 From NLM.

(7) Knudsen, A. M.; Halle, B.; Cédile, O.; Burton, M.; Baun, C.; Thisgaard, H.; Anand, A.; Hubert, C.; Thomassen, M.; Michaelsen, S. R.; et al. Surgical resection of glioblastomas induces pleiotrophin-mediated self-renewal of glioblastoma stem cells in recurrent tumors. *Neuro Oncol* **2022**, *24* (7), 1074-1087. DOI: 10.1093/neuonc/noab302 From NLM.

(8) Piroth, M. D.; Gagel, B.; Pinkawa, M.; Stanzel, S.; Asadpour, B.; Eble, M. J. Postoperative radiotherapy of glioblastoma multiforme: analysis and critical assessment of different treatment strategies and predictive factors. *Strahlenther Onkol* **2007**, *183* (12), 695-702. DOI: 10.1007/s00066-007-1739-5 From NLM.

(9) Smith, G. L.; Smith, B. D. Radiation treatment in older patients: a framework for clinical decision making. *J Clin Oncol* **2014**, *32* (24), 2669-2678. DOI: 10.1200/jco.2014.55.1168 From NLM.

(10) Rønning, P. A.; Helseth, E.; Meling, T. R.; Johannesen, T. B. A population-based study on the effect of temozolomide in the treatment of glioblastoma multiforme. *Neuro Oncol* **2012**, *14* (9), 1178-1184. DOI: 10.1093/neuonc/nos153 From NLM.

(11) Gavas, S.; Quazi, S.; Karpiński, T. M. Nanoparticles for Cancer Therapy: Current Progress and Challenges. *Nanoscale Res Lett* **2021**, *16* (1), 173. DOI: 10.1186/s11671-021-03628-6 From NLM.
(12) Wongpinyochit, T.; Johnston, B. F.; Seib, F. P. Manufacture and Drug Delivery Applications of Silk Nanoparticles. *J Vis Exp* **2016**, (116). DOI: 10.3791/54669 From NLM.
(13) Zhang, M.; Gao, S.; Yang, D.; Fang, Y.; Lin, X.; Jin, X.; Liu, Y.; Liu, X.; Su, K.; Shi, K. Influencing factors and strategies of enhancing nanoparticles into tumors in vivo. *Acta Pharmaceutica Sinica B* **2021**, *11* (8), 2265-2285. DOI: https://doi.org/10.1016/j.apsb.2021.03.033.
(14) Aldape, K. D.; Ballman, K.; Furth, A.; Buckner, J. C.; Giannini, C.; Burger, P. C.; Scheithauer, B. W.; Jenkins, R. B.; James, C. D. Immunohistochemical Detection of EGFRvIII in High Malignancy Grade Astrocytomas and Evaluation of Prognostic Significance. *Journal of Neuropathology & Experimental Neurology* **2004**, *63* (7), 700-707. DOI: 10.1093/jnen/63.7.700 (acccessed 10/21/2022).
(15) Pelloski, C. E.; Ballman, K. V.; Furth, A. F.; Zhang, L.; Lin, E.; Sulman, E. P.; Bhat, K.; McDonald, J. M.; Yung, W. K. A.; Colman, H.; et al. Epidermal Growth Factor Receptor Variant III Status Defines Clinically Distinct Subtypes of Glioblastoma. *Journal of Clinical Oncology* **2007**, *25* (16), 2288-2294. DOI: 10.1200/JCO.2006.08.0705 (acccessed 2022/10/20).
(16) Johnson, H.; Del Rosario, A. M.; Bryson, B. D.; Schroeder, M. A.; Sarkaria, J. N.; White, F. M. Molecular characterization of EGFR and EGFRvIII signaling networks in human glioblastoma tumor xenografts. *Mol Cell Proteomics* **2012**, *11* (12), 1724-1740. DOI: 10.1074/mcp.M112.019984 From NLM.
(17) Bonavia, R.; Inda, M. M.; Vandenberg, S.; Cheng, S. Y.; Nagane, M.; Hadwiger, P.; Tan, P.; Sah, D. W.; Cavenee, W. K.; Furnari, F. B. EGFRvIII promotes glioma angiogenesis and growth through the NF-κB, interleukin-8 pathway. *Oncogene* **2012**, *31* (36), 4054-4066. DOI: 10.1038/onc.2011.563 From NLM.
(18) Choi, B. D.; O'Rourke, D. M.; Maus, M. V. Engineering Chimeric Antigen Receptor T cells to Treat Glioblastoma. *J Target Ther Cancer* **2017**, *6* (4), 22-25. From NLM.
(19) Debinski, W.; Obiri, N. I.; Powers, S. K.; Pastan, I.; Puri, R. K. Human glioma cells overexpress receptors for interleukin 13 and are extremely sensitive to a novel chimeric protein composed of interleukin 13 and pseudomonas exotoxin. *Clin Cancer Res* **1995**, *1* (11), 1253-1258. From NLM.
(20) Sharma, P.; Debinski, W. Receptor-Targeted Glial Brain Tumor Therapies. *Int J Mol Sci* **2018**, *19* (11). DOI: 10.3390/ijms19113326 From NLM.
(21) Zeng, J.; Zhang, J.; Yang, Y. Z.; Wang, F.; Jiang, H.; Chen, H. D.; Wu, H. Y.; Sai, K.; Hu, W. M. IL13RA2 is overexpressed in malignant gliomas and related to clinical outcome of patients. *Am J Transl Res* **2020**, *12* (8), 4702-4714. From NLM.
(22) Sattiraju, A.; Solingapuram Sai, K. K.; Xuan, A.; Pandya, D. N.; Almaguel, F. G.; Wadas, T. J.; Herpai, D. M.; Debinski, W.; Mintz, A. IL13RA2 targeted alpha particle therapy against glioblastomas. *Oncotarget* **2017**, *8* (26), 42997-43007. DOI: 10.18632/oncotarget.17792 From NLM. Brown, C. E.; Warden, C. D.; Starr, R.; Deng, X.; Badie, B.; Yuan, Y. C.; Forman, S. J.; Barish, M. E. Glioma IL13Rα2 is associated with mesenchymal signature gene expression and poor patient prognosis. *PLoS One* **2013**, *8* (10), e77769. DOI: 10.1371/journal.pone.0077769 From NLM.

(23) Thaci, B.; Brown, C. E.; Binello, E.; Werbaneth, K.; Sampath, P.; Sengupta, S. Significance of interleukin-13 receptor alpha 2-targeted glioblastoma therapy. *Neuro Oncol* **2014**, *16* (10), 1304-1312. DOI: 10.1093/neuonc/nou045 From NLM.
(24) Brown, C. E.; Alizadeh, D.; Starr, R.; Weng, L.; Wagner, J. R.; Naranjo, A.; Ostberg, J. R.; Blanchard, M. S.; Kilpatrick, J.; Simpson, J.; et al. Regression of Glioblastoma after Chimeric Antigen Receptor T-Cell Therapy. *N Engl J Med* **2016**, *375* (26), 2561-2569. DOI: 10.1056/NEJMoa1610497 From NLM.
(25) Sampson, J. H.; Heimberger, A. B.; Archer, G. E.; Aldape, K. D.; Friedman, A. H.; Friedman, H. S.; Gilbert, M. R.; Herndon, J. E., 2nd; McLendon, R. E.; Mitchell, D. A.; et al. Immunologic escape after prolonged progression-free survival with epidermal growth factor receptor variant III peptide vaccination in patients with newly diagnosed glioblastoma. *J Clin Oncol* **2010**, *28* (31), 4722-4729. DOI: 10.1200/jco.2010.28.6963 From NLM. Brown, C.; Starr, R.; Naranjo, A.; Wright, C.; Bading, J.; Ressler, J. Adoptive transfer of autologous IL13-zetakine+ engineered T cell clones for the treatment of recurrent glioblastoma: lessons from the clinic. *Mol Ther* **2011**, *19* (suppl 1), S136-S137.
(26) Masliantsev, K.; Pinel, B.; Balbous, A.; Guichet, P. O.; Tachon, G.; Milin, S.; Godet, J.; Duchesne, M.; Berger, A.; Petropoulos, C.; et al. Impact of STAT3 phosphorylation in glioblastoma stem cells radiosensitization and patient outcome. *Oncotarget* **2018**, *9* (3), 3968-3979. DOI: 10.18632/oncotarget.23374 From NLM. Lo, H. W.; Cao, X.; Zhu, H.; Ali-Osman, F. Constitutively activated STAT3 frequently coexpresses with epidermal growth factor receptor in high-grade gliomas and targeting STAT3 sensitizes them to Iressa and alkylators. *Clin Cancer Res* **2008**, *14* (19), 6042-6054. DOI: 10.1158/1078-0432.Ccr-07-4923 From NLM.
(27) See, A. P.; Han, J. E.; Phallen, J.; Binder, Z.; Gallia, G.; Pan, F.; Jinasena, D.; Jackson, C.; Belcaid, Z.; Jeong, S. J.; et al. The role of STAT3 activation in modulating the immune microenvironment of GBM. *J Neurooncol* **2012**, *110* (3), 359-368. DOI: 10.1007/s11060-012-0981-6 From NLM.
(28) Fu, W.; Hou, X.; Dong, L.; Hou, W. Roles of STAT3 in the pathogenesis and treatment of glioblastoma. *Front Cell Dev Biol* **2023**, *11*, 1098482. DOI: 10.3389/fcell.2023.1098482 From NLM.
(29) Weathers, S. P.; de Groot, J. VEGF Manipulation in Glioblastoma. *Oncology (Williston Park)* **2015**, *29* (10), 720-727. From NLM.
(30) Xiao, Q.; Yang, S.; Ding, G.; Luo, M. Anti-vascular endothelial growth factor in glioblastoma: a systematic review and meta-analysis. *Neurological Sciences* **2018**, *39* (12), 2021-2031. DOI: 10.1007/s10072-018-3568-y.
(31) Gerstner, E. R.; Sorensen, A. G.; Jain, R. K.; Batchelor, T. T. Anti-vascular endothelial growth factor therapy for malignant glioma. *Curr Neurol Neurosci Rep* **2009**, *9* (3), 254-262. DOI: 10.1007/s11910-009-0037-2 From NLM.
(32) Arya, K. R.; Bharath Chand, R. P.; Abhinand, C. S.; Nair, A. S.; Oommen, O. V.; Sudhakaran, P. R. Identification of Hub Genes and Key Pathways Associated with Anti-VEGF Resistant Glioblastoma Using Gene Expression Data Analysis. *Biomolecules* **2021**, *11* (3). DOI: 10.3390/biom11030403 From NLM.
(33) Xiao, Q.; Yang, S.; Ding, G.; Luo, M. Anti-vascular endothelial growth factor in glioblastoma: a systematic review and meta-analysis. *Neurol Sci* **2018**, *39* (12), 2021-2031. DOI: 10.1007/s10072-018-3568-y From NLM.
(34) Mi, Y.; Smith, C. C.; Yang, F.; Qi, Y.; Roche, K. C.; Serody, J. S.; Vincent, B. G.; Wang, A. Z. A Dual Immunotherapy Nanoparticle Improves T-Cell Activation and Cancer

Immunotherapy. *Adv Mater* **2018**, *30* (25), e1706098. DOI: 10.1002/adma.201706098 From NLM.
(35) Rockwood, D. N.; Preda, R. C.; Yücel, T.; Wang, X.; Lovett, M. L.; Kaplan, D. L. Materials fabrication from Bombyx mori silk fibroin. *Nature Protocols* **2011**, *6* (10), 1612-1631. DOI: 10.1038/nprot.2011.379.
(36) Shaidani, S. Nanoparticle Formulation. Tufts University: 2022.
(37) Hasturk, O.; Sahoo, J. K.; Kaplan, D. L. Synthesis and Characterization of Silk Ionomers for Layer-by-Layer Electrostatic Deposition on Individual Mammalian Cells. *Biomacromolecules* **2020**, *21* (7), 2829-2843. DOI: 10.1021/acs.biomac.0c00523 From NLM.
(38) Oliveira, J. P.; Prado, A. R.; Keijok, W. J.; Antunes, P. W. P.; Yapuchura, E. R.; Guimarães, M. C. C. Impact of conjugation strategies for targeting of antibodies in gold nanoparticles for ultrasensitive detection of 17β-estradiol. *Sci Rep* **2019**, *9* (1), 13859. DOI: 10.1038/s41598-019-50424-5 From NLM.
(39) Shaidani, S. Characterization of Silk Nanoparticles. Tufts University: 2022.
(40) Zou, S.; Tong, Q.; Liu, B.; Huang, W.; Tian, Y.; Fu, X. Targeting STAT3 in Cancer Immunotherapy. *Molecular Cancer* **2020**, *19* (1), 145. DOI: 10.1186/s12943-020-01258-7.
Carmeliet, P. VEGF as a key mediator of angiogenesis in cancer. *Oncology* **2005**, *69 Suppl 3*, 4-10. DOI: 10.1159/000088478 From NLM.
(41) dos Santos, T.; Varela, J.; Lynch, I.; Salvati, A.; Dawson, K. A. Quantitative assessment of the comparative nanoparticle-uptake efficiency of a range of cell lines. *Small* **2011**, *7* (23), 3341-3349. DOI: 10.1002/smll.201101076 From NLM.

APPENDICES
PROJECT WEBSITE: Click Here!
PROJECT TIMELINE: Click Here!

Appendix 1: Project Schedule

Aims	Sub-Aims	Completion	September	October	November	December	January	February	March	April	May
Define Project		**100**									
1st Biweekly Report		**100**									
Antibody Lit Review	Choose Antibody for Targeting Research	**100**									
Silk Processing		**100**									
Silk Nanoparticles		**100**									
2nd Biweekly Report		**100**									
Cell Culture Training		**50**									
Technical Proposal Report Draft		**100**									

Project Presentations		**100**									
Preparing Nanoparticles		**100**									
Start Website	Add in Home Page, People Sections, References, and Project Update	**100**									
3rd Biweekly Report		**100**									
Risk Assessment Analysis		**100**									
Update Website	Update Project Section and References	**100**									
4th Biweekly Report		**100**									
Update Website	Update Project Section and References	**100**									
Project Presentations		**100**									
Finalized Web Site		**100**									
Technical Report		**100**									
Order Materials Necessary for Antibody Conjugation		**100**									
Make silk		**100**									
Make nanoparticles		**100**									
Biweekly Report #5		**100**									
Start EDC-NHS of IL-4		**100**									
ELISAs of IL-4 conjugated antibody		**100**									
K-12 Poster		**100**									
Mid Semester Presentation		**100**									
Biweekly Report #6		**100**									
Dual Conjugation of EDC-NHS of anti-pStat3 and anti-rVEGF		**100**									
Fluorescence of dual conjugated anti-pStat3 and anti-rVEGF nanoparticles		**100**									

Create new batch of silk NPs		**100**									
Biweekly Report #7		**100**									
Singular EDC-NHS of IL-13Rα2 & EGFRviii	*waiting on antibody delivery										
Fluorescence of IL-13Rα2 & EGFRviii nanoparticles	*waiting on antibody delivery										
Dual Conjugation of EDC-NHS of IL-13Rα2 & EGFRviii	*waiting on antibody delivery										
Fluorescence of dual conjugated IL-13Rα2 & EGFRviii nanoparticles	*waiting on antibody delivery										
Biweekly Report #8		**100**									
Final technical poster presentations		**100**									
Final web site		**100**									
Final technical report		**100**									

Appendix 2: Antibody Decision Matrix

Consideration	**Weight**	**IL-13Rα2**	**EGFRviii**	**EPHA2**
Expression in healthy tissue	5	3	5	3
Presence in GBM cells	5	5	3	4
Relevance/available background info	1	5	5	3
		45	**45**	**38**

Appendix 3: Project Design Chart

Characteristic	**Target Value**	**Why This Value**	**How We Will Test**
Nanoparticle size	100-120 nm	Appropriate size for entering tumors via leaky vasculature and for tumor cell uptake	DLS/SEM imaging
Nanoparticle	**TBD** → enough	Throughout various	FTIR Analysis,

antibody expression	to have efficient uptake in GBM cells	experiments, we will determine the target value for nanoparticle antibody expression based on which values optimize cellular uptake	Fluorescence microscopy with secondary antibody
Silk concentration	6%	6% silk has been determined by past studies to result in 100-120 nm particles	Concentration calculations by weighing 1000ul of silk solution, leaving overnight in 60°C oven, and weighing remaining silk
Uptake efficiency	**TBD** → enough to have efficient uptake in GBM cells	This value will be dependent on the various experiments we conduct to test nanoparticle antibody expression uptake efficiency (uptake is changed a lot by cell line & nanoparticle size[41])	FITC and lysosomal fluorescent microscopy or flow cytometry
Cell receptor expression	Cells express one of each receptor	This is important to test the efficacy of dual antibody conjugation, making sure both biomarkers are expressed whether we transfect cells with both, or receive IL-13Rα2 cells and transfect with EGFRviii	Flow cytometry and/or Western blot

Appendix 4: Risk Analysis

Item Number		**Risk Analysis**							**Risk Control**					**Risk/Benefit Analysis**
	Process Function/Requirement	HAZARD (Potential cause of Hazard/Potential Failure Mode)	HARM (Potential adverse effect/Potential effect of failure)	Potential causes/mechanisms of failure	Currnet Process Controls - Prevention, Detection	SEVERITY	OCCURRENCE	RPN	RISK MITIGATION	SEVERITY	OCCURRENCE	RPN	Risk reduced as far as possible (afap)?*	Benefits Outweigh Risks? (Yes/No)*
1	***Conjugation***	*Poor conjugation efficacy of antibodies (EPHa2 and IL-13Rα2) to silk nanoparticles*	*Process: off target targeting due to lack of specificity*	*EDC/NHS failure*	*Flow cytometry*	4	3	12	*Ensure EDC/NHS protocol being followed*	4	2	8	*afap*	*Yes*

									is correct						
2	***Reproducibility of silk batch***	*Inconsistent nanoparticle size and molecular weight*	*Process: cellular uptake ability and potential skewing of data*	*pH of deionized water too acidic, cross contamination of equipment in the silk processing room*	*Sterilization of equipment before use*	2	4	8	*Check pH of water before use*	2	2	4	*afap*	*Yes*
3	***Accuracy of testing***	*Poor accuracy of machine used during silk nanoparticle conjugation*	*Process: inconsistent silk size and MW across samples*	*DLS machine failure*	*Calibrating machine*	2	4	8	*Purchase a new DLS machine as this one may be broken*	2	2	4	*afap*	*Yes*
4	***Patient Receptor Expression***	*Patient doesn't express IL-13Rα2 or EphA2 receptors*	*Off-targeted binding due to lack of specific receptors*	*Patient genetics*	*Checking tumor cells first to see what is being expressed in the patient*	4	2	8	*Test only on patients that express both receptors through initial screenings*	4	1	4	*afap*	*Yes*
5	***Patient Targeting***	*IL-13Rα2 and EphA2 attack other areas expressing receptors of interest*	*Off-targeted binding due to expression on healthy tissue*	*Healthy tissue receptor expression*	*Choosing receptors that have low healthy tissue expression*	4	4	16	direct injection could decrease off target responses	4	2	8	*afap*	*Yes*
FINAL	Overall Residual Risk is Acceptable (Yes/No):														*Yes*

Appendix 5: Methods (Extended)

Silk Processing[35]

Silk concentration calculation:

1. Weigh an empty weigh boat (W1)
2. Add 1 mL silk solution (measured accurately with a 1000uM micropipette) and record the weight (W2)
3. Leave the weigh boat in a 60°C oven overnight
4. Next day, weigh the weigh boat again (W3)
5. The concentration of the silk solution (w/v) is:
   % = (W3-W1/W2-W1) x 100

Silk Nanoparticles[36]

Nanoparticle concentration calculation:

1. Weigh an empty weigh boat (W1)
2. Add 1 mL nanoparticle solution (measured accurately with a 1000uM micropipette) and record the weight (W2)
3. Leave the weigh boat in a 60°C oven for a few hours
4. Weigh the weigh boat again (W3)
5. The concentration of the nanoparticle solution (w/v) is:
   % = (W3-W1/W2-W1) x 100

EDC/NHS[37]

EDC/NHS calculations:

1. EDC ratio is 500 silk fibroin (SF) to 124 EDC
2. NHS ratio is 500 SF to 40 NHS
    a. Use these ratios to determine how many mg each of EDC and NHS is needed to perform the protocol, respectively
3. Based on the silk concentration, 3.1 mL of buffer per 500 mg of silk is needed
    a. This ratio will help to determine the amount of MES in uL needed to be added in each respective EDC and NHS jar

Antibody	
SF	500 mg
Antibody	166 mg
EDC	124 mg
NHS	40 mg

Ultracentrifugation[37]

Spin 1:

1. Turn on the ultracentrifuge machine
2. Make sure the settings of the ultracentrifuge are 60K, 30 minutes, at 4°C
3. Grab two sealing tubes and fill them equally with the EDC/NHS nanoparticle solution
4. Fill the tubes with DI water to the lip of the tube, leaving the cylinder at the top empty for the stopper and cap
5. Weigh tubes and make sure they are within 0.01g to 0.02g of each other
6. Place tubes into centrifuge rotor balanced (e.g. one in hole 2 and one in hole 6)
7. Screw on the lid of the rotor and place onto the slit in a ultracentrifuge, pressing down on the silver center button to lock the two together (spin to make sure the rotor is calibrated)
8. Close the lid of the machine, and start the vacuum by pressing the vacuum button
9. Wait until the vacuum is 0 microns and the temperature is close to 4°C (around 6°C to 7°C) to start the machine

After Spin 1:

1. Before opening the ultracentrifuge, turn off the vacuum once it reaches 0 microns
2. Take out tubes from the rotor (if stuck, use a pipette tip and tweezers)
3. Remove supernatant around nanoparticle pellet using an 18G needle and syringe
4. Save supernatant in a 15 mL tube, label, and store in the freezer
5. Resuspend nanoparticle pellet in 3 mL of DI water using an 18G needle and syringe

Spin 2:

1. Repeat **Spin 1** steps 4-9

After Spin 2:

1. Repeat **After Spin 1** steps 1-5, label the supernatant tube

Spin 3:

1. Repeat **Spin 1** steps 4-9

After Spin 3:

1. Repeat **After Spin 1** steps 1-4
2. Instead of resuspending the pellet, soak the pellet in 1 mL of DI water
3. Store sealing tubes in the freezer

Secondary Antibody Tagging[38]

1. Thaw nanoparticles and supernatant at room temperature
2. Resuspend nanoparticles in a sealing tube, combine both tubes into a 15 mL tube and add DI water to make a 10 mL solution
3. Sonicate nanoparticle solution at 30% for 30 seconds twice
4. Obtain an arbitrary 4 mL solution containing:
    a. Antibody nanoparticles or supernatant
    b. Blocking butter (for nanoparticles only) → 0.2% BSA (blocking buffer solution)
    c. Secondary antibody (IL-4 has a concentration of 2 mg/mL)
5. Grab six 15 mL tubes
    a. Tube 1 (antibody nanoparticle with secondary):
        i. 4 mL solution in total
        ii. Use 3 mL antibody-tagged nanoparticle solution
        iii. Calculate the concentration of secondary antibody:
            1. $\frac{2\ mg/mL * 4mL}{2000\ microgram/mL}$ = 4 µg/mL
        iv. Calculate the concentration of the blocking buffer solution
            1. Want 0.2% of 4 mL to be blocking buffer: 8 µL
        v. Fill the rest of the solution with DI water to make 4 mL
            1. In this case, 988 µL
    b. Tubes 2, 3, and 4 (supernatants with secondary)
        i. 3 mL of supernatant (each tube will be a different supernatant)
        ii. 4 µL of secondary antibody
        iii. Fill will DI water until 4 mL solution
            1. In this case, 996 µL
    c. Tube 5 (blank nanoparticles with secondary)
        i. 4 mL solution in total
        ii. Use 3 mL blank nanoparticle solution
        iii. Calculate the concentration of secondary antibody:
            1. $\frac{2\ mg/mL * 4mL}{2000\ microgram/mL}$ = 4 µg/mL
        iv. Calculate the concentration of the blocking buffer solution
            1. 1 mL solution: 900µL of DI water, 100 µL BSA
            2. Want 0.2% of 4 mL to be blocking buffer: 8 µL
        v. Fill the rest of the solution with DI water to make 4 mL
            1. In this case, 988 µL
    d. Tube 6 (blocking buffer)
        i. 1 mL solution: 900 µL of DI water, 100 µL BSA
6. Shake all tubes on a stir plate covered in tin foil (since the secondary is light sensitive) for 2 hours
7. Ultracentrifuge both nanoparticle tubes (Tube 1 and Tube 5) 3 times following the **Ultracentrifugation** protocol

Imaging

1. Retrieve a 96-well plate
2. Create a standard curve with 12 standards
    a. In this experimental case, wanted 8 µg/mL of antibody, so created a 1 mL solution with the secondary of a concentration of 2 mg/mL giving 4 µL secondary antibody out of the 1 mL solution
    b. Each standard is 200 µL of the first standard combined with 200 µL of DI water
3. Fill all 12 wells of the first row with 200 µL of each standard
4. Fill the first 3 wells of the second row with 200 µL of the 1º + 2º antibody NPs
5. Fill the first 3 wells of the third, fourth, and fifth rows with 200 µL of supernatants 1-3
6. Fill the first 3 wells of the sixth row with 200 µL of blank nanoparticles
7. Fill the first 3 wells of the seventh row with 200 µL of blank NPs + secondary antibody
8. Take the 96-well plate to the plate reader to quantify the fluorescence of the secondary antibody
    a. Press the blue button in the top left corner to open the plate holder
    b. Place plate in with no lid
    c. Press the blue button to close the plate holder and close the face of the machine
    d. Log into the desktop and open the software
    e. Set up a schematic of the plate reader on software by blocking out which wells have a solution in them
    f. Run read and save data to an excel file
9. Take the 96-well plate to the Keyence fluorescence microscope to visualize the secondary binding
    a. Turn on the desktop and log onto the Keyence software
    b. Open Keyence and orient the well plate to match the setup on the software
    c. Image well plate at an exposure of 1-6
    d. Save images

Colocalization Analysis:

1. Follow along with this youtube video: https://www.youtube.com/watch?v=4umlxVsjY04 to find the areas of each channel and their overlap
2. Divide the area of the overlap by the area of one channel (A) for the percent colocalization of antibody A with antibody B
3. Divide the area of the overlap by the area of the other channel (B) for the percent colocalization of antibody B with antibody A